Impact in Agriculture

Impaxon

Article

Field Evaluation of a Mechanically Synchronized Aeration-Fertilization Machine for Turfgrass Management

Mutlaq Farhan Alsubaie [1], H. N. Abdelmageed [1], M. M. Kasem [2] and M. M. Abohabaga [1, *]

[1] Agricultural Engineering Department, Faculty of Agriculture, Mansoura University, Mansoura, 35516, Egypt
[2] Department of Vegetables and Floriculture, Faculty of Agriculture, Mansoura University, Mansoura, 35516, Egypt

* Correspondence: mm_abohabaga@mans.edu.eg (M.M.A)

Abstract

The Combined Aeration/Fertilization Unit (CAFU) was designed to allow turf aeration and fertilizer application in a single operation; both would be accomplished with this single machine, using solid steel fork tines (1.5 cm diameter) to penetrate the soil to a maximum depth of 12 cm. This method of soil aeration has been successfully tested using solid tines, which increase the soil's physical properties after aeration when compared to pre-aeration conditions; bulk density (1.70 to 1.40 g/cm3), total void ratio (0.559 to 0.893), and total porosity (35.85 to 47.17%) were all improved after aeration. The increase in porosity and decrease in bulk density would help to improve water and air infiltration into the soil, creating more optimal soil conditions in the root zone. The 50% reduction in penetration resistance indicates that soil compaction was relieved through aeration. The CAFU's fertilizer placement accuracy was 85%, and the average radial deviation was only 3 cm. This accuracy is attributed to mechanical synchronization between the aeration drum and the fertilizer gate, which enabled precise placement of fertilizer into the aeration holes. The field capacity of the CAFU is 0.643 feddans/h (2.7 km/h), with a fuel consumption of 5.5 L/h and a specific energy consumption of 23.67 kWh/fed. The CAFU presents a technical approach to integrating both operations to improve soil physical properties and ensure accurate, efficient fertilizer application. The developed CAFU embodies a pragmatic engineering methodology for turfgrass management and establishes a foundation for subsequent assessments in varied field environments.

Keywords: Combined machine; Turfgrass; Fertilizing rate; Specific energy; Soil aeration; Soil compaction

Citation: Alsubaie, M. F., Abdelmageed, H. N., Kasem, M. M., & Abohabaga, M. M. (2026). Field Evaluation of a Mechanically Synchronized Aeration-Fertilization Machine for Turfgrass Management. *Impact in Agriculture* 2026, **2**, 4. https://doi.org/10.65500/agriculture-2026-004

Received: 2 April 2026 | Revised: 10 May 2026 | Accepted: 15 May 2026 | Published: 23 May 2026

1. Introduction

Aeration of soil is one of the most important practices for maintaining a healthy turfgrass site because it improves the soil's physical properties (i.e., pore space), aids root establishment, and enhances nutrient cycling [1], [2] When aeration and fertigation are combined, fertigation is more efficient in using fertilizer and water and results in better turfgrass quality and quantity [3], [4]. Additionally, combining aeration and fertigation creates optimal conditions for root growth, protects soil structure from damage, reduces evaporation of water from the soil surface, and reduces nutrient loss from the soil [5], [6]. For roots to respire, microorganisms to be active, and nutrient cycling to occur, aerobic conditions (oxygen levels) must be present in the soil. Aeration also promotes greater oxygen diffusion into the soil, which increases beneficial soil bacterial growth and nutrient cycling, thereby enhancing plant growth [7-9]. Studies have demonstrated that soil aeration increases overall soil bacterial diversity, thereby improving ecological processes related to nitrogen turnover and soil fertility [10], [11]. Furthermore, from an environmental standpoint, integrated fertilization and aeration practices will minimize or eliminate nutrient leaching and reduce the risk of water pollution by providing sustainable, environmentally friendly turfgrass management systems [3], [12]. In addition to agronomic and environmental benefits, the use of these combined practices will result in substantial reductions in labor, energy, and equipment costs [13], [14].

Mechanical aeration technologies have been extensively developed to create cavities within the soil profile, increasing total pore volume and reducing compaction, primarily in intensively managed turfgrass systems. Samples and Sorochan [15] and Kansas State University [16] report that mechanical aeration helps create perforations that enable gas exchange, increase infiltration capacity, and facilitate root penetration through the compacted surface layer of soil. Typical mechanical aeration methods include core aeration (hollow or solid tines), slit or slice aeration, spike aeration, shatter core aeration, and vertical cutting. Core aeration methods are much better than slice or spike aeration at alleviating soil compaction and thatch accumulation, and they cause less soil damage while still providing efficient aeration [17], [6]. Solid tine aeration is achieved by inserting rigid steel tines into the soil. Solid-tine aeration increases pore space by creating vertical perforations throughout the soil profile without disrupting the soil surface, unlike hollow-tine core aeration. Therefore, this type of aeration is especially well-suited for turf and ornamental grass areas that require minimal disruption to the soil surface [18], [19]. Although solid tine aeration can significantly reduce surface compaction and increase oxygen diffusion, its effects are only temporary and have been found ineffective at alleviating deep-seated compaction problems or inadequate aeration resulting from excessive irrigation [19], [20]. Mechanical penetration can damage turfgrass roots, increasing the turfgrass's susceptibility to root disease under certain conditions [21].

Selecting an aeration method is difficult because it involves balancing relief from compaction, improved soil aeration, efficient operation, and minimal surface disturbance on managed turf [17], [22]. There has been extensive research on soil fertilization and aeration. However, to date, little research has examined how to mechanically combine the two operations into a single implement, particularly in turfgrass management. Earlier research measured aeration and fertilization separately, rather than treating them as a single coordinated/mechanized process. Combining aerating and fertilizer application in a single machine reduces labor, fuel use, and operating time by reducing the number of field passes.

Hence, this study aimed to develop and evaluate a combined prototype that simultaneously aerates and fertilizes during a single pass over turfgrass.

2. Materials and Methods

The experiment was conducted at Mansoura University in Dakahlia Governorate, Egypt, during the 2025 season to assess the operational effectiveness of a machine specifically designed to aerate turfgrass. This experiment was executed in sandy clay soil, which compacts, preventing roots from growing normally and reducing the amount of air and moisture that can pass through the root zone. The experimental field was divided into plots measuring 30 m in length and 1 m in width. The experiments were conducted on turf established with the Paspalum grass variety because it can withstand significant mechanical stress during the growing season.

To achieve stable and consistent operating conditions, the Combined Aeration and Fertilization Unit (CAFU) was mounted on a tractor and operated at a steady forward speed of 2.7 km/h to ensure uniform field conditions. The apparatus had robust fork tines with a 1.5 cm diameter, achieving a penetration depth of 12 cm. These design criteria facilitated the efficient disruption of compacted soil strata and resulted in changes in soil physical properties, including increased porosity and void ratio.

Combined turfgrass aeration and fertilization unit (CAFU)

The developed combined aeration–fertilization prototype consists of two main units, namely the aeration and the fertilization units, as illustrated in Figure 1. These two units are mechanically linked through a transmission system consisting of a chain and two gears, increasing the rotation of the fertilizer rotor by a ratio of 4 times, which ensures synchronized and stable operation of the machine's components during field work. The unit also includes two land wheels used solely for mobility during transport to the field. These wheels are removed during operation to allow direct contact between the drum and the soil, ensuring effective aeration.

Aeration unit

The aeration module comprises a hollow cylindrical drum constructed from low-carbon steel, including a wall thickness of 4 mm, a length of 1000 mm, and an outer diameter of 400 mm. The drum is mounted on a central shaft by high-precision ball bearings to enable optimal rotation with minimal friction. The drum surface has 20 heavy-duty steel tines, evenly spaced across the drum in 4 long lines. Each line of five tines is spaced vertically apart by 20 cm; each has a diameter of 1.5 cm and a length of 12 cm, and all tines are mounted at right angles (90°) to the drum so that they will penetrate soil effectively and uniformly.

The drum turns because of the tractor's forward movement, and the tines create sufficient friction against the soil to produce enough torque on the drum, given its rotational inertia, so that it turns with the tractor once it has developed sufficient torque. The way the tines are regularly spaced around the drum's circumference creates a dynamic balance that reduces vibrations and provides greater stability at high speeds. When using the tines, the depth of soil penetration equals the tine length (12 cm) (Figure 1).

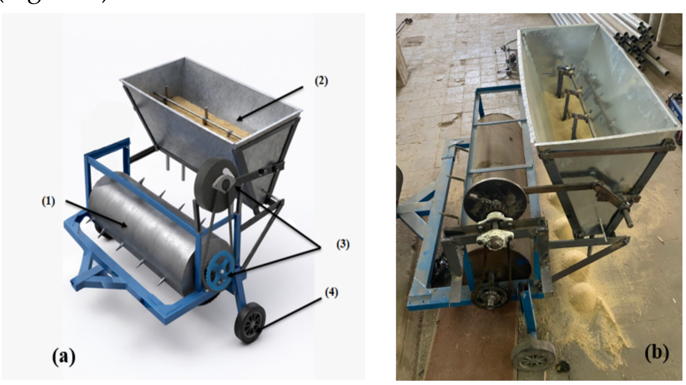

Figure 1. The combined aeration and fertilization unit (CAFU): (a) components of the CAFU: (1) aeration unit, (2) fertilization unit, (3) gear reduction system, and (4) movement wheel; (b) photograph of the manufactured unit.

- The fertilization unit

The fertilizer hopper is placed above the aeration drum, with a deliberate horizontal offset from the drum's vertical axis and has a truncated-pyramid design (100 cm × 45 cm × 48 cm). This design ensures granular fertilizer's gravity-driven flow while reducing the risk of bridging by using a wall inclination that exceeds the internal friction angle of the material (Figure 2). The base of the hopper contains five circular outlets, each connected to a vertical downspout and spaced to correspond to the tine spacing, with just enough longitudinal offset to account for the soil penetration pattern. In this manner, applying fertilizer through outlets near the rhizosphere improves nutrient use efficiency by delivering nutrients directly to where they can be used.

The metering gate in the hopper controls fertilizer release by intermittently discharging it to match the aeration drum's tine spacing and timing. The metering gate's movement is mechanically linked to the aeration drum through a constant ratio transmission (1:4). The rotary motion transmitted to the smaller gear will then be transmitted to a flywheel-crank mechanism, which will change continuous rotary motion into reciprocating motion and then transmit that reciprocating motion through a connecting linkage to actuate the metering gate. The metering gate, therefore, has periodic opening and closing cycles. The operating principle of the above system depends entirely on mechanical synchronism. A crank's angular velocity is decreased to one-quarter of the forward speed by the 1:4 transmission ratio to produce one-quarter of the output drum speed because the output drum was divided geometrically into four functional segments for the tine rows. Each quarter revolution of the output drum completes one cycle through the full open/close metering gate. This allows the metered fertilizer to discharge simultaneously with the tines, creating new soil cavities and ensuring accurate fertilizer placement (Figure 2).

This unique rotary-to-reciprocating motion conversion approach is one of the key innovations of this system. It permits precise timing between the application of metered fertilizer and soil aeration, applying solely mechanical control with no need for electronic components. In the field trial, test plots measuring 30 m × 1.0 m were created (Figure 3), with a tractor operating at an average forward speed of 2.73 km/h (0.75 m/s). The elapsed time to complete the experimental area was measured using a stopwatch and included the time the test machine was operating during this trial.

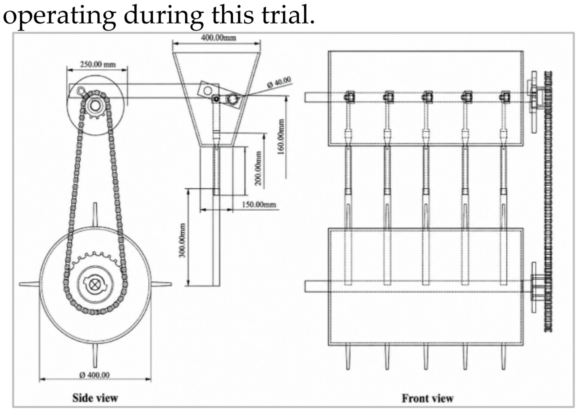

Figure 2. Gear system for rotational speed amplification and motion transmission in the machine.

Figure 3. Field evaluation showing aeration holes made during the experimental plot (1 m × 30 m)

- The power source

The tractor used for this research was a 2010 Kubota model equipped with a four-cylinder diesel engine (No. 74192) with a displacement of 2600 cm^3. The tractor provides a rated power of 18.3 kW and has a dry mass of 1070 kg. The chassis number is E06245.

- Measurements: Soil moisture content

The soil's moisture content was assessed using an electric oven set to 105°C for 24 hours. Soil samples were collected from the field by conducting various turfgrass aeration operations, with three replicates per sample. Moisture content was measured using the oven-dry weight method, as follows in Eq. (1):

$$S_m = \frac{W - W_1}{W} \tag{1}$$

Where: W: weight of soil sample before drying, g, W1: weight of the same soil sample after drying, g.

- Soil bulk density

Soil samples were collected using a cylindrical core (100 cm^3 volume). The core samples were immediately weighed and then dried at 105°C for 24 hours. Soil bulk density was determined according to Eq. (2):

$$\rho b = \frac{W_d}{T_v} \tag{2}$$

Where: ϱb: Soil bulk density, g/cm^3, Wd: Dry soil mass, g, Tv: Total soil volume, cm^3.

Soil porosity

Soil porosity was determined according to Eq. (3):

$$S_p = \left(1 - \left(\frac{\rho b}{\rho s}\right)\right) \times 100 \tag{3}$$

Where: Sp: Soil porosity (%), ϱs: Real soil density, g/cm^3.

Void ratio

Void ratio (e) was calculated using Eq. (4):

$$e = \frac{\rho s - \rho b}{\rho b} \tag{4}$$

- Penetration resistance

Soil penetration resistance was determined according to Eq. (5):

$$PR = \frac{F \times 9.81}{A \times 10^3} \tag{5}$$

Where: PR: Penetration resistance, kPa, F: Force required for penetration, kg, A: Average cone area, m^2.

Actual field capacity

The actual field capacity (AFC) of the machine was calculated according to Aboegela et al. [23], as follows in Eq. (6):

$$AFC = \frac{A}{T} \tag{6}$$

Where: AFC = Actual field capacity (fed/h), A = Area covered during the test (fed), T = Total operating time, including turning, maneuvering, and filling the fertilizer tank

- Hole density

Hole density produced by the aeration drum was estimated based on the drum circumference and the total number of tines installed on the drum. The number of holes produced per unit area was determined according to UASDA [24], as follows in Eq. (7):

$$HD = \frac{N}{C \times W} \tag{7}$$

Where: HD = Hole density (holes/m^2), N = Number of tines on the drum, C = Drum circumference (m), W = Effective working width (m)

Transmission from the aeration drum to the fertilizer gate.

The fertilizer feeding gate is actuated by a crank mechanism mechanically linked to the aeration drum via a gear transmission with a speed-increase ratio of 1:4. The drum's rotary motion is converted into the gate's reciprocating motion.

With a crank radius of r = 0.2 m, the linear displacement of the gate is expressed as follows in Eq. (8):

$$x\,dt = r\cos(\omega_c t) \tag{8}$$

Where: ω_c is the angular velocity of the crank after speed amplification, given by Eq. (9):

$$\omega_c = 4\omega_d = \frac{4V}{R} \tag{9}$$

, with V as the tractor forward speed and R the drum radius. The instantaneous linear velocity of the gate is calculated according to Eqs. 10 and 11:

$$v(t) = -r\omega_c \sin(\omega_c t) \tag{10}$$

The maximum linear velocity occurs at $\sin(\omega_c t) = \pm 1$

$$v_{max} = r \cdot \omega_c \tag{11}$$

Energy requirements

The required engine power was estimated according to Embaby (1985), as follows in Eq. (12):

$$EP = [f.c \times \left(\frac{1}{3600}\right) \times \rho f \times L.C.V \times 427 \times \eta_{th} \times \eta_m \times \frac{1}{75} \times \frac{1}{1.36}] \tag{12}$$

Where: EP: Engine power, kW, $f.c$: Fuel consumption, L/h, ρ_f: Density of diesel fuel (0.85 kg/L), L.C.V: Lower calorific value of diesel fuel (10000 kcal/kg), 427: Thermo-mechanical equivalent (kg.m/kcal), ηth: Thermal efficiency of diesel engine (35%), ηm: mechanical efficiency of diesel engine (80%)

- Specific energy requirement

The specific energy consumed during operation was calculated by relating the required engine power to the effective field capacity according to Usaborisut and Prasertkanthe [26], as follows in Eq. (13):

$$SE = \frac{Ep}{AFC} \tag{13}$$

Where: SE = Specific energy consumption (kW·h/fed), EP = Engine power (kW), AFC = Actual field capacity (fed/h)

- Fertilizer application rate

The fertilizer application rate was determined based on the quantity of fertilizer discharged during the test area and extrapolated to one feddan according to Sui [27], as follows in Eq. (14):

$$Fr = \frac{Q}{A} \tag{14}$$

Where: Fr = Fertilizer application rate (kg/fed), Q = Quantity of fertilizer applied during the test (kg), A = Experimental area (fed)

Distribution accuracy and deviation measurements

The fertilizer placement accuracy relative to the aeration holes was evaluated by measuring the deviation between the target hole center and the actual fertilizer deposition center. The measurements were conducted using a Cartesian coordinate system to determine the horizontal and vertical displacement between the two points.

The horizontal deviation (Δx) and vertical deviation (Δy) were calculated according to Gao et al. [28], as follows in Eqs. 15 and 16:

$$\Delta x = | x_{actual} - x_{target} | \tag{15}$$

$$\Delta y = | y_{actual} - y_{target} | \tag{16}$$

Where: Δx = horizontal deviation (cm), Δy = vertical deviation (cm), xactual, yactual = coordinates of the actual fertilizer deposition point, xtarget, ytarget = coordinates of the target aeration hole center, the radial error (Er), which represents the direct distance between the target point and the actual fertilizer deposition point, was calculated using the Pythagorean Theorem as follows:

The radial deviation between the target point (aeration hole center) and the actual fertilizer deposition point was calculated using the Pythagorean theorem as follows in Eq. (17):

$$E_r = \sqrt{\left(x_{actual} - x_{target}\right)^2 + \left(y_{actual} - y_{target}\right)^2} \tag{17}$$

Where: E_r is the radial error (cm), y_{actual}, y_{target} are the coordinates of the actual fertilizer deposition point, and x_{actual}, x_{target} are the coordinates of the target aeration hole.

To obtain the overall distribution performance, the mean radial error was calculated as follows in Eq. (18):

$$\overline{E_r} = \frac{\sum_{i=1}^{n} E_{ri}}{n} \tag{18}$$

Where:$\overline{E_r}$ = mean radial error (cm), E_{ri} = radial error for each observation, n = number of observations (n = 45)

Finally, the distribution accuracy (A%) was estimated by relating the mean radial error to the row spacing distance used in the machine (20 cm), which represents the allowable reference spacing between aeration holes, as follows in Eq. (19):

$$A\,\% = \left(1 - \frac{\overline{E_r}}{Row\ spacing}\right) \times 100 \tag{19}$$

Where: A% = distribution accuracy (%), Row spacing = spacing between adjacent aeration holes (20 cm)

These calculations were used to quantify the precision of fertilizer placement relative to the aeration holes generated by the machine.

3. Results

3.1. Soil physical properties and the effect of mechanical aeration

A field study was conducted to evaluate the impact of the developed aeration machine on the physical properties of turfgrass soil. The assessment aimed to quantify changes in soil structure and porosity resulting from the use of solid tines with a 12 cm penetration depth and a 1.5 cm diameter. The results obtained were compared with the initial soil condition (control) to assess the effectiveness of the aeration process.

3.2. Mechanical and chemical characterization of the experimental soil

Before conducting the field experiments, the soil's fundamental physical and chemical properties were determined to ensure the reliability and accuracy of the results. The measured parameters are listed in Table 1.

Table 1. Chemical and physical properties of the trial soil

Property	**Value**
Coarse sand (%)	3.58
Fine sand (%)	29.41
Silt (%)	40.38
Clay (%)	26.63
Organic matter (%)	1.56
pH	8.13
Saturation percentage (SP, %)	52.9

Table 1 shows that the soil at this site is classified as sandy clay loam based on mechanical analyses. Due to the high proportions of silt (40.38%) and clay (26.63%) in the sample, the soil's compaction potential is relatively high. Compaction of the soil affects water infiltration, air exchange, and root depth, all of which impact root zone development. For these reasons, it has been determined that mechanical aeration will improve soil structure and porosity and create more favorable conditions within the root zone.

3.3. The influence of aeration on soil moisture content and bulk density

Table 2 shows that soil moisture content and bulk density changed before and after mechanical aeration. These two parameters are important factors in the soil's physical condition and compaction status.

Table 2. Soil moisture content and soil bulk density before and after mechanical aeration

Condition	**Moisture content (%)**	**Bulk density (g/cm^3)**
Before aeration (compacted condition)	17.50	1.70
After aeration (improved condition)	30.00	1.40

The effects of aeration resulted in an average reduction of soil bulk density from 1.70 g/cm^3 to 1.40 $g/cm^{3,}$ indicating that solid tines can create sufficient looseness in the soil structure to relieve the effects of compaction; previous studies have shown that mechanical aeration also has a significant effect on reducing soil bulk density. In addition, the soil moisture content (30.0%) has increased, thereby reducing resistance to tine penetration and allowing greater penetration into the soil profile.

3.4. Development of soil porosity and void ratio

Soil porosity and void ratio were calculated based on bulk density and an assumed particle density of 2.65 g/cm^3. The results are summarized in Table 3.

Table 3. Soil porosity and void ratio before and after aeration

Condition	**Porosity (%)**	**Void ratio**
Before aeration (compacted condition)	35.85	0.559
After aeration (improved condition)	47.17	0.893

An increase in the soil's total porosity was observed, from 35.85% to 47.17% after aeration. This improvement is expected to enhance air and water movement within the soil profile and reduce surface water accumulation. Additionally, the void ratio increased to 0.893, indicating a significant expansion in pore space. The increase in total porosity observed in the present study is consistent with previous studies reporting improvements in soil pore structure and porosity following mechanical treatments to alleviate soil compaction. Similar increases in soil porosity have been documented following vegetation-driven structural improvement [29], subsoiling [30], and pore-enhancing soil amendments [31], [32]. These studies attributed the observed improvements to increased pore development and enhanced soil structural conditions, which is in agreement with the results obtained in the present study.

3.5. Impact of aeration on soil penetration resistance

Soil penetration resistance is one of the most important physical indicators of soil compaction and of plant roots' ability to penetrate the soil and obtain water and nutrients. For this study, soil penetration resistance was measured before the development of the aeration machine, which was tested at a forward speed of 2.7 km/h and a penetration depth of 12 cm. The test results are listed in Table 4.

Table 4. Soil penetration resistance before and after aeration

Condition	Penetration resistance (kPa)
Before aeration (compacted condition)	1660
After aeration (50% improvement)	830

Results show that soil penetration resistance has been reduced by almost half (50%) with treatment using the aeration device, from 1660 kPa to 830 kPa. The decrease in penetration resistance indicates that the developed aeration machine effectively alleviated soil compaction by using solid tines that form vertical pathways and break up compacted soil layers.

Decreasing penetration resistance is expected to facilitate water and nutrient movement within the soil profile and may support conditions conducive to root development. The study further establishes that mechanical aeration plays an important role in improving soil physical conditions and reducing soil compaction.

3.6. Machine's specifications

The combined unit consists of a rotary steel drum with four rows of solid tines, each containing five hardened steel tines 1.5 cm in diameter, allowing them to penetrate the soil up to approximately 12 cm. The tines were spaced 20 cm apart within each row, giving the machine an effective working width of approximately 1 m.

Also, the machine had a rear-mounted fertilizer hopper with a capacity of 135 kg. It was mechanically connected to the aeration drum and, therefore, allowed fertilizer to be applied in time with the drilling operation. For these trials, a 1:2 (by weight) mix of NPK fertilizer and sand was used. With this setup, the farmer could drill and fertilize fields in a single operation, without first spreading fertilizer.

3.7. Mechanical linkage between the aeration drum and the metering gate

A field trial was performed to evaluate the aeration/fertilizer system with the following specifications: an aeration drum radius of 0.25 m and a tractor forward speed of 0.75 m/s (2.7 km/h). A kinematic analysis of the fertilizer metering gate's reciprocating motion caused by the crank mechanism (0.2 m crank length) showed that the gear transmission between the aeration drum and the crank provided a speed amplification ratio of 1:4. As a result of this speed amplification, the crank rotates four times faster than the aeration drum and therefore has an angular velocity of:

$$\omega_c = \frac{4 \times 0.75}{0.25} = 12\ rad/s$$

Then, the gate's maximum linear velocity is:

$$v_{max} = 0.2 \times 12 = 2.4\ m/s$$

The corresponding cycle time of the gate motion is:

$$T = \frac{2\pi}{\omega_c} = \frac{2\pi}{12} \approx 0.523\ m/s$$

3.8. Field capacity

The field trial was performed on a 30 m² (1.0 m × 30 m) test plot. The machine's forward speed was 2.7 km/h (≈0.75 m/s), taking approximately 40 seconds to cover the total working distance of 30 m over three runs covering the trial area.

The actual field capacity (AFC) was calculated according to the total operating time as:

$$AFC = \frac{0.01428 fed}{0.0111 h} \approx \frac{0.643 fed}{h}$$

3.9. Hole density

The aeration cylinder's circumference was 3.14 × 0.4 m = 1.257 m, with 20 cylinders rotating. From this configuration, each cylinder has 20 holes per revolution. Therefore, the machine produced an approximate density of perforations per cylinder:

$$\frac{20}{1.257 \times 1} = 15.9 \ \approx 16\ holes/m^2$$

This density suffices to perforate soil and promote aeration, gas exchange, and the movement of water/nutrients through the root zone.

3.10. Fuel consumption and power requirement

The combined unit's penetration depth is 12 cm, and the tractor's fuel consumption rate is about 5.5 L/h. The required engine power can be determined using the formula provided by Embaby [25]:

The required engine power was determined according to Embaby [25]:

$$EP = \left[5.5 \times \left(\frac{1}{3600}\right) \times 0.85 \times 10000 \times 427 \times 0.35 \times 0.80 \times \frac{1}{75} \times \frac{1}{1.36}\right] = 15.22\ kW$$

3.11. Specific energy requirement

The specific energy of the developed machine was determined by dividing the required engine power by the actual field capacity.

The calculated specific energy requirement was:

$$\frac{15.22\ kW}{0.643\ fed/h} = 23.670\ kW.h/fed$$

3.12 Fertilizer application rate

Applying aeration and fertilization separately is less efficient and agronomically inferior to coordinating the two. The benefits of aeration are site-specific, timing-sensitive, and not consistently strong on their own, whereas fertilization is most effective when rate, timing, and placement match turf demand [33-35].

The fertilizer discharge rate was determined using the experimental plot dimensions and the calibrated output per aeration hole. Calibration results showed that each aeration hole received approximately 31 g of the NPK fertilizer–sand mixture (1:2 by weight).

The experimental plot dimensions were 30 m × 1 m (L × W), with a total area of 30 m². The spatial distribution of aeration holes within the plot was structured such that each 10 m length contained 32 rows, with 5 holes per row. Therefore, the number of holes per 10 m segment was determined as follows:

$$N_{10} = R \times H_r = 32 \times 5 = 160\ holes$$

Given the total plot length of 30 m, which is equivalent to three 10 m segments, the total number of aeration holes in the entire plot (N_Total) was:

$$N_{total} = N_{10} \times S = 160 \times 3 = 480\ holes$$

where S is the number of 10 m segments (3).

The total mass of fertilizer applied per plot (Mtotal) was then calculated by multiplying the number of holes by the mass per hole (mhole = 31 g):

$$480 \times 31 = 14880g = 14.88\ kg$$

The fertilizer application rate per unit area (Rarea) was subsequently obtained by dividing the total fertilizer mass by the plot area (A = 30 m²):

$$R_{area} = \frac{M_{total}}{A} = \frac{14.880}{30} = 0.469\ kg/m^2$$

This application rate reflects the actual distribution achieved by the mechanical synchronization system under the specified experimental conditions, providing a quantitative reference for field-scale fertilization operations using the developed aeration–fertilization machine.

3.13. Fertilizer placement accuracy

Forty-five sampling points distributed across the experimental area were assessed to evaluate the spatial accuracy of fertilizer placement relative to the aeration holes (Table 1). The coordinates of the actual fertilizer deposit and the center of the target aeration hole were recorded for each point, and the horizontal deviation (dx), vertical deviation (dy), and radial error (Er) were calculated. The total area of the experimental plot was 30 m² (30 × 1 m), and 45 sampling points were uniformly distributed to represent the target fertilizer deposition centers generated by the synchronized fertilization system. The trial was uniformly divided into three longitudinal bands, each 1 m wide, representing the machine's effective working width and the target fertilization sites, given the timing system used. The diagram of the mechanical gate system used in this experiment shows the distance traveled (2.7 km/h) with the implement wandering as required (Maneuvers) at either end of the longitudinal strips, which were used to define the Actual Field Capacity. The spatial distribution of samples should assess the mechanical equipment's ability to accurately place fertilizer into the pre-formed aeration holes created by the solid tines (diameter = 1.5 cm; depth = 12 cm).

According to the measured data, the total radial error was 135 cm, yielding a mean radial error of about 3.0 cm.

The distribution accuracy (%) was calculated in relation to the spacing between adjacent aeration holes (20 cm):

$$A\,\% = \left(1 - \frac{3}{20}\right) \times 100 = 85\%$$

According to the distribution accuracy score (85%), there is a high level of precision in fertilizer application relative to aeration holes (i.e., hole spacing). This is due to the mechanical synchronization between the fertilizer gate mechanism and the rotating aeration drum, ensuring fertilizer is placed immediately after each hole is created.

In addition, deviations in both the x- and y-coordinates (number of soil samples collected within each zone) remain small. Therefore, the majority of the applied fertilizer does not reach areas beyond the effective influence zone of the aeration holes. Because fertilizer is placed near the aeration holes, nutrient availability within the plant root zone is expected to increase. Therefore, fertilizer will be utilized more efficiently within turfgrass systems.

3.14. Spatial accuracy analysis

Comparison of deviations and radial errors across three measurement groups

Table 5 presents the average spatial deviations of fertilizer placement nearly the same distance from the correct location throughout the three sections of the trials conducted (horizontal – dx) (vertical - dy). There was a minor variation in the average absolute deviation for both horizontal and vertical measurements across all segments; therefore, the machine's functionality remained constant across all operating distances.

The average vertical distance from a reference point directly beneath the gate to the fertilizer application point (average radial distance) ranged from approximately 3.04 cm (Segment 1) to 3.28 cm (Segment 3), with an overall average of approximately 3.18 cm. Thus, since there was such a minor variation in radial distance amongst the three segments, the system studied produced consistent accuracy in distribution regardless of the distance at which it was operated.

The consistency in the average radial error was due to the solid synchronization of the mechanical systems of the combined aeration drum and fertilizer gate. Therefore, the fertilizer discharge was controlled and equal in amount from one discharge to another. Since the overall average radial error was small in relation to the distance between the fertilizer application points, a majority of the fertilizer drops landed sufficiently close to the application point, as illustrated in Table 5.

Table 5. Average spatial deviations and radial error of fertilizer placement across experimental segments

Segment	dx (cm)	dy (cm)	Er (cm)
Segment 1 Avg.	2.27	2.15	3.04
Segment 2 Avg.	2.43	2.23	3.22
Segment 3 Avg.	2.41	2.26	3.28
Overall Avg.	2.37	2.21	3.18

Figure 4 presents a scatter plot showing the spatial deviation of actual points from their target coordinates across the three experimental segments. Target points made in gray and actual measurements are represented in color by segment: blue shows Segment 1 (0-10 m), green shows Segment 2 (10-20 m), and red shows Segment 3 (20-30 m). Each target point shows the difference between d_x and d_y from the target to the actual target point of measurement, as shown by the length of the arrows, which corresponds to the radial error Er.

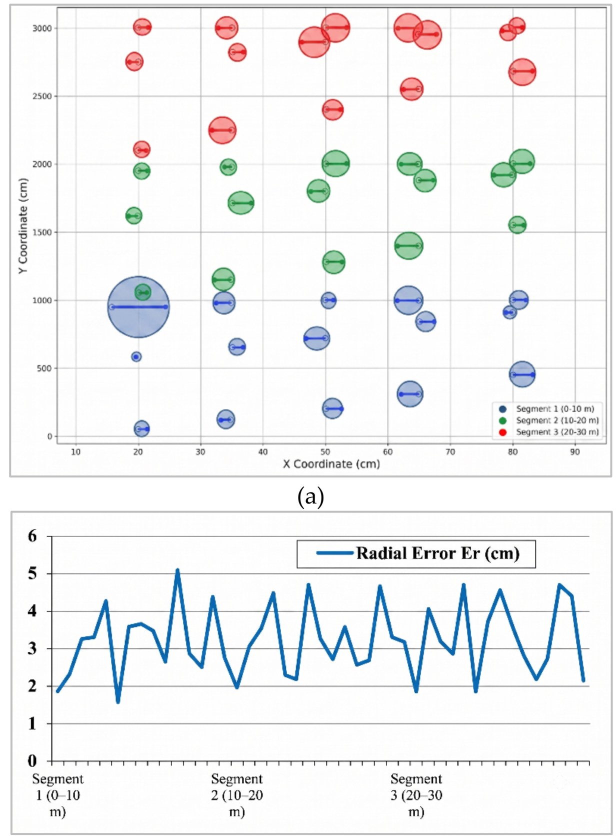

(a)

(b)

Figure 4. Scatter plot of spatial deviation (a) and radial error (Er) (b) for fertilization points across the three trial segments.

From the data plot, the deviations are within 5 cm, showing high overall precision of the machine in achieving the planned point locations. The smaller deviation values for Segment 1 show greater consistency regarding consistent machine operation in the beginning of the experiment, versus Segment 2 or Segment 3, where deviations are greater in magnitude and occur at multiple points, possibly representing minor cumulative errors from either a slight drift in the machine trajectory or variability of the soil across the experimental area.

The 85% distribution accuracy provides reasonable confidence that placing fertilizer relative to the aeration holes approximately maximizes the precision of aeration and fertilization systems. The mechanical synchronization between the aeration system's rotating drum and the fertilizer gate ensures fertilizer is discharged immediately after each aerated hole is formed. Aeration has been recognized as a time-intensive management practice [36], [37], and willingness to adopt it has been reported to be partly a function of the time and labor demands associated with its implementation. When aeration and fertilization are performed as separate operations, extra field passes, labor, and management activities are needed. Previous studies have shown that aeration can improve water infiltration and nutrient movement within the soil profile, and that aeration, coupled with nutrient application, may reduce runoff and nutrient export under certain conditions [38-40]. Thus, in the absence of aeration during fertilization, some of these potential benefits may not be achieved. Furthermore, nitrogen losses in turf systems are highly sensitive to fertilizer source, application rate, and timing, irrigation practices, and turf growth stage, which means that fertilizer applications that are not synchronized with favorable growth and soil conditions can increase the risk of nutrient leaching [35], [41], [42]. It is also known that root development and nutrient uptake can be restricted by soil compaction and poor aeration. However, aeration does not always result in prompt improvements, as temporary declines in turf quality following aerification have been reported, followed by subsequent recovery [37], [19], [43]. The results of this study indicate that turfgrass management programs may need to consider the timing and coordination of aeration and fertilization practices. The developed aeration–fertilization unit demonstrated the capability to combine both operations in a single pass, addressing the operational difficulties of performing aeration and fertilization separately while maintaining constant fertilizer placement relative to the soil penetration points. Small spatial deviations observed during operation indicate reliable synchronization between the aeration and fertilizer delivery mechanisms, confirming the effectiveness of the developed design for localized nutrient application.

3.15. Statistical Analysis of Radial Error (Er)

The results of the one-way ANOVA showed that there is not any statistically significant ($P>0.05$) difference in mean radial experiment segment errors (Er) for segments 1 through 3 ($P=0.784$) (Table 6). Mean Er for segments 1, 2, and 3 are 3.04 cm, 3.22 cm, and 3.28 cm, respectively; and the maximum Er difference among segments is 0.24 cm. In addition to the F-value being low ($F=0.245$), the variation of segment means was smaller than the variation observed within segments. The radial error ranges of the three experimental segments show substantial overlap, indicating similar placement performance throughout the experimental plot. Thus, the aeration and fertilization prototype developed and tested in this study maintained a consistent relationship between soil perforation and fertilizer discharge over the 30 m operating distance. While the average Er increased between segments one and three, the increase was not statistically significant and remained within the expected range of normal variability.

An average radial error of 3.18 cm indicates that the fertilizer was placed at an acceptable distance from the target aeration holes. Variations in E r could be due to field-related factors, such as differences in soil at each site and/or slight variations in the machine's movement. Overall, the statistical analysis demonstrated spatially consistent fertilizer placement performance across the evaluated experimental segments.

Table 6. Analysis of variance (ANOVA) for radial error (Er) among the experimental segments

Source of Variation	Between Segments	Within Segments (Error)	Total
Degrees of Freedom (DF)	2	42	44
Sum of Squares (SS)	0.468	40.120	40.588
Mean Square (MS)	0.234	0.955	–
F-value	0.245	–	–
P-value	0.784	–	–

4. Conclusion

The combined machine integrated aeration and fertilization into a single pass, combining both operations into a single field operation. Use of 1.5 cm-diameter solid fork tines at an operating depth of 12 cm produced significant improvements in soil physical properties. Bulk density decreased from 1.70 g/cm3 pre-aeration to 1.40 g/cm3 post-treatment. Total soil porosity increased from 35.85% to 47.17%, and void ratio increased from 0.559 to 0.893. The machine was very effective at alleviating soil compaction; penetration resistance decreased by 50% from 1660 kPa pre-aeration to 830 kPa post-aeration. The mechanical synchronization between the aeration drum and the fertilizer distribution system achieved an average distribution accuracy of 85% and an average radial deviation of 3 cm. In operation, the machine produced a field capacity of 0.643 fed/h at a forward speed of 2.7 km/h, with a fuel consumption rate of 5.5 L/h and a specific energy requirement of 23.670 kWh/fed. The research shows that combining mechanical aeration and fertilization improves soil physical properties and reduces soil compaction, while providing accurate fertilizer placement within or near the aeration holes. The developed prototype demonstrates the technical feasibility of integrating aeration and fertilizer application into a single operation and represents a practical engineering approach for turfgrass management. In addition, the evaluation primarily focused on the mechanical performance of the aeration–fertilization system and the precision of fertilizer placement relative to the aeration holes, whereas long-term agronomic responses, such as turfgrass growth, root development, nutrient-use efficiency, and changes in soil properties, were not investigated. Future research should evaluate the machine at different soil textures, operating speeds, tine settings, and fertilizer compositions. Additional research is also recommended to assess the long-term impacts of synchronized aeration and fertilization on turfgrass performance, soil physical properties, and overall nutrient management efficiency under field conditions.

Author Contributions: M.F.A., H.N.A., M.M.K., and M.M.A. contributed equally to the conceptualization, methodology, investigation, formal analysis, data curation, writing, and validation of this study. All authors have read and approved the final manuscript.

Funding: This research received no external funding.

Institutional Review Board Statement: Not applicable.

Informed Consent Statement: Not applicable.

Data Availability Statement: Data are available from the corresponding author upon reasonable request.

Acknowledgments: Not applicable.

Conflicts of Interest: The authors declare no conflicts of interest.

AI Use Declaration: Generative AI was used solely for language editing and proofreading. The authors reviewed and approved all content and take full responsibility for the manuscript.

References:

1. Y. Li, J. Wang, Y. Du, and Q. Chen, "Optimization of an aerated fertilizer irrigation application scheme for tomato photosynthesis, yield and quality in Xi'an, China," *Scientia Horticulturae*, vol. 338, Art. no. 113743, 2024, https://doi.org/10.1016/j.scienta.2024.113743.
2. Y. Sun, L. Duan, H. Zhong, H. Cai, J. Xu, and Z. Li, "Effects of irrigation-fertilization-aeration coupling on yield and quality of greenhouse tomatoes," *Agricultural Water Management*, vol. 299, Art. no. 108893, 2024, https://doi.org/10.1016/j.agwat.2024.108893.
3. T. Głąb, W. Szewczyk, K. Gondek, M. Mierzwa-Hersztek, J. Palmowska, and K. Nęcka, "Optimization of turfgrass fertigation rate and frequency," *Agricultural Water Management*, vol. 234, Art. no. 106107, 2020, https://doi.org/10.1016/j.agwat.2020.106107.
4. D. McFadden and J. D. Fry, "Aerification effects on 'Innovation' Zoysiagrass in 2020–2022," *Kansas Agricultural Experiment Station Research Reports*, vol. 9, 2023, https://doi.org/10.4148/2378-5977.8482.
5. D. M. Williams, C. M. Straw, A. P. Smith, K. L. Watkins, S. G. Hong, W. F. Floyd, and B. M. Wyatt, "Using electromagnetic induction to inform precision turfgrass management strategies in sand capped golf course fairways," *Agrosystems, Geosciences & Environment*, vol. 7, Art. no. 70020, 2024, https://doi.org/10.1002/agg2.70020.
6. C. Isom and C. Thompson, "Effects of within event aerator pass frequency and tine size on sand incorporation and organic matter accumulation in cool season putting greens of the Pacific Northwest," *Crop, Forage & Turfgrass Management*, vol. 12, Art. no. 70104, 2025, https://doi.org/10.1002/cft2.70104.
7. Z. Yu, H. Wang, D. Yu, N. Yin, and J. Zhang, "The effect of aeration and irrigation on the improvement of soil environment and yield in dryland maize," *Frontiers in Plant Science*, vol. 15, Art. no. 1464624, 2024, https://doi.org/10.3389/fpls.2024.1464624.
8. Q. Bian, Z. Dong, Y. Zhao, Y. Feng, Y. Fu, Z. Wang, J. Zhu, and L. Ma, "Micro-/nanobubble oxygenation irrigation enhances soil phosphorus availability and yield by altering soil bacterial community abundance and core microbial populations," *Frontiers in Plant Science*, vol. 15, Art. no. 1497952, 2025, https://doi.org/10.3389/fpls.2024.1497952.
9. Y. Liang, M. Wu, J. Zhang, Z. Ma, Y. Han, Y. Wen, R. Chen, J. Liu, H. Li, and Z. Wang, "Synergy between aerated drip and biodegradable film enhances sustainable maize production in arid oasis," *European Journal of Agronomy*, vol. 165, Art. no. 127535, 2025, https://doi.org/10.1016/j.eja.2025.127535.
10. Z. Qian, S. Zhuang, J. Gao, L. Tang, J. D. Harindintwali, and F. Wang, "Aeration increases soil bacterial diversity and nutrient transformation under mulching induced hypoxic conditions," *Science of the Total Environment*, vol. 817, Art. no. 153017, 2022, https://doi.org/10.1016/j.scitotenv.2022.153017.
11. Z. Xiao, H. Lei, Y. Lian, Z. Zhang, H. Pan, C. Yin, and Y. Dong, "Impact of aerated drip irrigation and nitrogen application on soil properties, soil bacterial communities and agronomic traits of cucumber in a greenhouse system," *Plants*, vol. 12, no. 22, Art. no. 3834, 2023, https://doi.org/10.3390/plants12223834.
12. S. Vijayakumar, G. Srikrishan, D. Sudheer, and M. H. Chandrakant, "Drip and fertigation technology to enhance water and nutrient use efficiency in semi arid region," *Journal of Krishi Vigyan*, vol. 12, pp. 477–484, 2024, https://doi.org/10.5958/2349-4433.2024.00087.9.
13. A. Fares and F. Abbas, "Irrigation systems and nutrient sources for fertigation (SCM 25)," Univ. of Hawaiʻi at Mānoa, 2009. [Online]. Available: https://www.haifa-group.com/sites/default/files/2024-03/SCM-25.pdf
14. C. Neff, "Exploring the benefits of fertigation," *USGA Green Section Record*, vol. 62, 2024. [Online]. Available: https://www.usga.org/content/usga/home-page/course-care/green-section-record/62/issue-08/exploring-the-benefits-of-fertigation.html
15. T. Samples and J. Sorochan, "Turfgrass maintenance: Cultivation (W161 B)," Univ. of Tennessee Institute of Agriculture, 2023. [Online]. Available: https://utia.tennessee.edu/publications/wp-content/uploads/sites/269/2023/10/W161-B.pdf
16. Kansas State University, "Cultivation and thatch control." [Online], 2019. Available: https://www.k-state.edu/turf/resources/lawn-problem-solver/maintenance/cultivation/
17. P. J. Brown, J. L. Atkinson, L. B. McCarty, and V. L. Quisenberry, "Soil physical responses of a compacted sports field following various core aerification techniques," *International Journal of Plant & Soil Science*, vol. 9, pp. 1–9, 2016, https://doi.org/10.9734/IJPSS/2016/21694.
18. A. J. Turgeon and J. E. Kaminski, *Turfgrass Management*. Turfpath LLC, 2019.

19. C. M. Straw, R. A. Grubbs, G. M. Henry, R. N. Carrow, and V. Cline, "Long-term effect of open-spoon aerification on plant and soil properties of community level sports fields," *Crop, Forage and Turfgrass Management*, 2016, https://doi.org/10.2134/cftm2016.04.0031.
20. L. R. J. Hubbard, L. B. McCarty, V. L. Quisenberry, and P. J. Brown, "Aerification strategies affecting golf green subsurface properties," *International Journal of Agriculture Research and Environmental Sciences*, vol. 4, pp. 1–14, 2023, https://doi.org/10.51626/ijares.2023.04.00028.
21. R. W. Smiley, P. H. Dernoeden, and B. B. Clarke, Eds., *Compendium of Turfgrass Diseases*, 3rd ed. APS Press, 2005, https://doi.org/10.1094/9780890546154.
22. N. R. Amgain, C. H. Fontanier, and D. L. Martin, "Short term effects of alternative cultivation practices on putting green infiltration rates," *Crop Science*, vol. 61, pp. 4425–4435, 2021, https://doi.org/10.1002/csc2.20604.
23. M. A. Aboegela, M. Elmeadawy, M. Okasha, M. A. Orabi, and N. E. Mansour, "Developing a pesticide spraying machine suitable for grape orchards," *Progress in Agricultural Engineering Sciences*, 2026, Art. no. 446, https://doi.org/10.1556/446.2026.00304.
24. University of Arkansas System Division of Agriculture, "Calibrating drills and broadcast planters for small seeded forages (FSA3111)," 2019. [Online]. Available: https://www.uaex.uada.edu/publications/pdf/FSA-3111.pdf
25. A. T. Embaby, "A comparison of the different mechanization system for career crop production," M.Sc. thesis, Faculty of Agriculture, Cairo Univ., Cairo, Egypt, 1985.
26. P. Usaborisut and K. Prasertkan, "Specific energy requirements and soil pulverization of a combined tillage implement," *Heliyon*, vol. 5, Art. no. e02757, 2019, https://doi.org/10.1016/j.heliyon.2019.e02757.
27. R. Sui, "Performance assessment of a variable rate fertilizer applicator," *Journal of Agricultural Science*, vol. 11, pp. 25–30, 2019, https://doi.org/10.5539/jas.v11n2p25.
28. J. Gao, F. Zhang, J. Zhang, H. Zhou, and T. Yuan, "Development and field performance evaluation of hole fertilizing planter and dynamic alignment control system for precision planting of corn," *Precision Agriculture*, vol. 25, pp. 1189–1212, 2023, https://doi.org/10.1007/s11119-023-09988-6.
29. H. Chen, S. He, Z. Xue, X. Zhang, K. Yu, K. Wang, A. Ren, J. Han, X. Zhao, X. Zhu, C. Liu, L. Hong, and J. Xing, "Halophytes reclamation soil through improving soil structures, decreasing salinity and enhancing SOC storage in coastal saline land," *Ecological Engineering*, vol. 223, Art. no. 107860, 2026, https://doi.org/10.1016/j.ecoleng.2025.107860.
30. J. Liu, T. Clough, S. Carrick, J. Luo, A. Podolyan, N. Wells, C. Chisholm, J. Shen, P. Li, L. Du, H. Pan, L. Zhang, and H. J. Di, "Subsoiling reduces N_2O emissions by altering the relative gas diffusivity, O_2 status and microbial communities in grazed pasture soil," *Geoderma*, vol. 467, Art. no. 117716, 2026, https://doi.org/10.1016/j.geoderma.2026.117716.
31. Q. Yu, M. Wang, Y. Tian, X. Shi, X. Li, L. Xu, X. Xie, Y. Shi, and Y. Zhu, "Effects of porous clay ceramic rates on aeration porosity characteristics in a structurally degraded soil under greenhouse vegetable production," *Pedosphere*, vol. 31, no. 4, pp. 606–614, 2021, https://doi.org/10.1016/S1002-0160(21)60006-1.
32. X. Ma Chen, B., Wang, S., Shao, L., Cao, Y., Xu, X., ... & Zhao, L, "Organic amendments enhance saline-alkali soil organic carbon capacity: A perspective on soil Fe speciation and salt-tolerant bacteria," Chemical Engineering Journal, 2026, https://doi.org/10.1016/j.cej.2026.176997.
33. R. O. Maguire, P. J. A. Kleinman, C. J. Dell, D. B. Beegle, R. C. Brandt, J. M. McGrath, and Q. M. Ketterings, "Manure application technology in reduced tillage and forage systems: A review," *Journal of Environmental Quality*, vol. 40, no. 2, pp. 292–301, 2011, https://doi.org/10.2134/jeq2009.0228.
34. R. O. Carey, G. J. Hochmuth, C. J. Martinez, T. H. Boyer, V. D. Nair, M. D. Dukes, G. S. Toor, A. L. Shober, J. L. Cisar, L. E. Trenholm, and J. B. Sartain, "A review of turfgrass fertilizer management practices: Implications for urban water quality," *HortTechnology*, vol. 22, no. 3, pp. 280–291, 2012, https://doi.org/10.21273/HORTTECH.22.3.280.
35. L. Barton and T. D. Colmer, "Irrigation and fertiliser strategies for minimising nitrogen leaching from turfgrass," *Agricultural Water Management*, 2006, https://doi.org/10.1016/j.agwat.2005.07.011.
36. M. Popp, K. Lindsay, A. J. Ashworth, P. A. Moore Jr., P. R. Owens, T. C. Adams, M. Welch, B. Roark, D. Pote, and J. Pennington, "Economic and GHG emissions changes of aeration and gypsum application," *Agriculture, Ecosystems & Environment*, vol. 321, Art. no. 107616, 2021, https://doi.org/10.1016/j.agee.2021.107616.
37. J. L. Atkinson, L. B. McCarty, and W. C. Bridges, "Effect of core aerification frequency area impacted and topdressing rate on turf quality and soil physical properties," *Agronomy Journal*, 2012, https://doi.org/10.2134/agronj2012.0224.
38. S. P. Bhattarai, N. Su, and D. J. Midmore, "Oxygation unlocks yield potentials of crops in oxygen-limited soil environments," *Advances in Agronomy*, 2005, https://doi.org/10.1016/S0065-2113(05)88008-3.
39. D. M. Butler, D. H. Franklin, M. L. Cabrera, A. S. Tasistro, K. Xia, and L. T. West, "Evaluating aeration techniques for decreasing phosphorus export from grasslands receiving manure," *Journal of Environmental Quality*, vol. 37, no. 3, pp. 1279–1287, 2008, https://doi.org/10.2134/jeq2007.0289.
40. S. B. Shah, J. L. Miller, and T. J. Basden, "Mechanical aeration and liquid dairy manure application impacts on grassland runoff water quality and yield," *Transactions of the American Society of Agricultural Engineers*, 2004. 47(3): pp. 777-788. https://doi.org/10.13031/2013.16109
41. A. M. Petrovic, "The fate of nitrogenous fertilizers applied to turfgrass," *Journal of Environmental Quality*, 1990, https://doi.org/10.2134/jeq1990.00472425001900010001x.
42. K. Guillard and K. L. Kopp, "Nitrogen fertilizer form and associated nitrate leaching from cool-season lawn turf," *Journal of Environmental Quality*, 2004, https://doi.org/10.2134/jeq2004.1822.
43. W. C. Tim Chamen, A. P. Moxey, W. Towers, B. Balana, and P. D. Hallett, "Mitigating arable soil compaction: A review and analysis of available cost and benefit data," *Soil and Tillage Research*, 2015, https://doi.org/10.1016/j.still.2014.09.011.